Journal of Crystal Growth 519 (2019) 91–99

Contents lists available at ScienceDirect

Journal of Crystal Growth

journal homepage: www.elsevier.com/locate/jcrysgro

Molecular aggregation of L-isoleucine in aqueous solution and its impact on the determination of solubility and nucleation kinetics

Nik Salwani Md Azmi[a], Nornizar Anuar[a,*], Kevin J Roberts[b], Noor Fitrah Abu Bakar[a], Nurul Fadhilah Kamalul Aripin[a]

[a] Faculty of Chemical Engineering, Universiti Teknologi MARA, 40450 Shah Alam, Selangor, Malaysia
[b] Centre for the Digital Design of Drug Products, School of Chemical and Process Engineering, University of Leeds, LS2 9JT, UK

ARTICLE INFO

Communicated by S. Veesler

Keywords:
A1. Measurement using dissolution and gravimetric methods
B1. Meta-stable zone widths
C1. Nucleation kinetics and mechanism
D1. Inter-molecular clustering
E1. Critical aggregate concentration
F1. 2-step nucleation

ABSTRACT

Comparison between the solubility of L-Isoleucine as measured using gravimetric and dissolution methods reveals significant differences which is consistent with the presence of solute aggregation in solution. Calculation of the critical aggregation concentration confirms this analysis revealing this concentration to lie between the two measured solubility values suggesting the existence of a stability zone roughly defined by the temperature/concentration range of 40 °C/33 g/L to 75 °C/42 g/L in which a mixture of free and aggregated molecules under the slurried conditions appear to exist. Dynamic light scattering result reveals that the aggregate size lies within the range of 40–170 nm. The potential impact of relying on the measurement of solubility using gravimetric data based on solution isolation of the slurried state for such systems is highlighted through a comparison of the values of representative crystallization parameters such as metastable zone width (MSZW) and nucleation kinetics as determined using solubilities derived from both methodologies. Reduction in solution pH in the aggregated molecular state is consistent with the aggregates being formed from neutral species suggesting, in turn, that this compound might crystallize via a 2-step nucleation process. This research suggests that caution should be exercised when using solubility data derived from gravimetric measurements particularly for amphiphilic molecules where solute ordering in solution might be expected.

1. Introduction

Solubility is the maximum amount of a given compound that can be freely dissolved in a solution when at equilibrium with its associated crystalline solid form at a certain temperature and pressure [1,2]. Solubility information is very important in designing solution crystallization processes for separation and purification purposes, especially in the pharmaceutical industry [3,4] where solubility is also a key parameter in determining the efficacy of drugs [5,6]. Solubility can be determined using many methods and the gravimetric method [7–10], in which the concentration of solute in the solution at the desired temperature is determined in the presence of excess solute in the solution, is widely used. Solubility can also be determined from polythermal crystal dissolution experiments, as measured as a function of constant solution heating rate [11–13]. To date, no attempt has been made to compare the solubility result between the gravimetric method and dissolution method, where the data directly affects the metastable zone region, and hence supersaturation calculation, which is crucial for the estimation of nucleation kinetics in crystallization process. Metastable zone is evaluated using temperatures derived from both solubility and crystallization data [14,15]. It is always assumed that the saturation temperature determined for solubility is the same regardless of the different methods used. Researchers have used either solubility data derived from gravimetric [7,16,17] or dissolution method [11–13] for kinetic evaluation without necessarily evaluating whether these two methods will provide different saturation temperatures, where the difference in saturation temperature reflects the amphiphilic behavior of a particular solute molecule and/or indicate a degree of solute aggregation within the solution state.

Generally, the molecules of hydrophobic compounds, when dissolved in water, can tend to self-assemble [18] forming aggregates, since water itself has high cohesive energy [19–22]. Molecular self-assembly in water can also result in monolayer formation at the water-air interface [19] with the hydrophobic groups of the molecules tending to 'escape' from the energetically unfavourable aqueous environment by protruding into the vapour phase above the water surface [23]. For a colloidal system at a concentration above the critical aggregation concentration (CAC) or solute ordering, the molecules can tend to self-

* Corresponding author.
E-mail address: nornizar@salam.uitm.edu.my (N. Anuar).

https://doi.org/10.1016/j.jcrysgro.2019.04.019
Received 29 October 2018; Received in revised form 26 March 2019; Accepted 18 April 2019
Available online 20 April 2019

assemble in solution [24], and aggregate together to form spherical micelles [25] with the hydrophobic group sheltered from the water by a mantle provided by hydrophilic groups. When the concentration of the aggregated phase increases, there is a possibility for such micelles to grow forming, e.g. cylindrical, vesicles, planar bilayer or inverted micelle structures depending on the nature of their inter-molecular packing [25] geometry and on the physico-chemical properties of the compound. The CAC can be determined by several methods including conductivity measurements, surface tension, fluorescence spectroscopy, foaming, voltammetry, scattering techniques, nuclear magnetic resonance spectroscopy and calorimetry [26].

L-isoleucine, the compound investigated in this study, is known to be the most hydrophobic amino acid (hydrophobic character of 1.83) and one which exists as zwitterions in solution [27,28]. The solubility of L-isoleucine in water has been previously studied by Zumstein & Rousseau [7], Anuar et al. [9] and Matsuo et al. [29] providing broadly similar results using the gravimetric method, suggesting that this method is indeed a reliable method. However, analysis of this material's solubility using dissolution method has been found [9] to give lower solubilities when compared to the solubility calculated using gravimetric data. Given the potential impact of inaccurate solubility data on the design of the crystallization process and its associated nucleation kinetics determination, further examination of these differences is clearly needed.

In this paper, the effects of data (temperature and concentration) extraction from both gravimetric and dissolution solubility methods on the assessment of the crystallizability and nucleation kinetics of L-isoleucine have been analyzed and compared with a view to assessing the origin of the high solubility determined using gravimetric method. Comparative analysis of analogous data from both dissolution and gravimetric experiments have not, to the authors' knowledge, been carried out and hence these differences in solubility have been investigated as a function of temperature, pH and solute concentration. Additionally, the critical aggregation concentration was also measured and this, together with dynamic light scattering measurements was used to quantify and rationalize the resulting analysis. Finally, a comparative analysis of the solubility and nucleation kinetics as derived from these two methods is provided in order to access their impact on crystallization.

2. Materials and methods

2.1. Material

L-isoleucine, molecular formula $C_6H_{13}O_2N$, molecular weight 131.2 and purity greater that 99.0%, was purchased from Merck. Distilled water was used to make up the solutions. L-isoleucine used in this work was a form A polymorph. L-isoleucine is a zwitterionic molecules consists of a carboxyl (COO^-) functional group, an amino (NH_3^+) functional group and an alkyl side chain. The molecular structure of L-isoleucine can be found in Supplementary Material, section S1.

2.2. Solubility determination

Solubility data using the gravimetric [7–9] method were taken from Anuar at el. [9], whilst its determination from dissolution [10] experiments, were carried out in a jacketed reactor with constant stirring provided by a retreat curve impeller and temperature regulated by a programmable refrigerated bath. In this, a known amount of L-isoleucine was added to 200 mL distilled water in the jacketed reactor at 25 °C and heated up to 85 °C for one hour at a rate of 0.7 °C/min. The experiments were carried out as a function of solute concentration of 21, 23, 25, 30, 35, 40 and 48 g/L. The dissolution process was carried out as a function of heating rate (0.7, 0.5, 0.25, and 0.1 °C/min) with the dissolution temperature being taken as that associated with the dissolution of the last crystal dissolved in the solution. In this work, the dissolution temperatures were detected by using eye visualization, in which the temperatures were noted when no more crystals were detected in the solution. The dissolution process was carefully and attentively observed, and each reading was repeated three times, with standard deviation for dissolution temperature between 0.1 °C and 0.8 °C. The dissolution temperature as a function of heating rate was extrapolated to zero rate which was taken as the equilibrium solubility temperature for a given concentration.

A description of the methodology used for gravimetric analysis is given in Supplementary Material (section S2). A comparison between the solubility parameters derived by the gravimetric and dissolution methods is given in Supplementary Material (section S3).

2.3. Critical aggregation concentration determination

The critical aggregation concentration (CAC) was determined [26,30] using a conductivity meter for concentrations from 20 g/L to 55 g/L and temperatures between 25 °C and 75 °C using the same jacketed reactor as described in 2.2. In this, a fixed amount of L-isoleucine was added to 100 mL of distilled water which was equilibrated for an hour after which the conductivity probe was inserted into the solution and the conductivity was measured.

2.4. Estimation of aggregate size and shape

Aggregation size measurements were carried out using dynamic light scattering (Malvern Zetasizer Nano ZS90). The sample was prepared by dissolving a known amount of L-isoleucine into 50 mL of distilled water, and following complete dissolution, the clear solution was drawn using a syringe and transferred into a clear disposable cell and analyzed. Each sample measurement was repeated three times and the aggregate size distribution was measured. The number of molecules in the aggregate, M was calculated as a function of aggregation size using Eq. (1) [20]:

$$M = \frac{4\pi R^2}{a_o} \tag{1}$$

where R is the radius of aggregate and a_0 is the polar surface area. For L-isoleucine, the polar surface area was taken to be 63.3 Å^2 [31]. The estimation of the type of aggregate formed (e.g. spherical micelles, inverted micelles, vesicles, etc.) was assessed through solution dilution experiments. In this, a solution (40 g/L at 50 °C) was diluted to a series of low concentration solutions (38, 36, 34 and 32 g/L) followed by measurement of the aggregation size of solute in solution.

2.5. Measurements of the species pKa and solution pH with respect to the presence of aggregates

L-isoleucine exists as a zwitterion molecule in solution, which means that the total charge on the molecule would be expected to change as a function of the solution pH depending on the molecular dissociation constants (pK_a) for the ionisable functional groups in the molecule. In this case, there are three possible L-isoleucine molecular species in solution, namely [RH^+], [RH^o] and [RH^-]. These represent cationic, neutral and anionic states, respectively which reflects the total molecule's charge they carry in the solution, which is due to inter-molecular proton transfer.

The values for pK_{a1}, and pK_{a2} were determined by using a standard procedure, in which an S curve was generated and the values of [RH^+], [RH^o] and [RH^-] were determined from the Henderson-Hasselbach equation [32] (derivation can be found in Supplementary Material, section S4). The pH of L-isoleucine solutions with a known aggregates size distribution was also measured using a 100 mL L-isoleucine solution of a known concentration and temperature with the combination of concentration and temperature selected for this experiment being based on the measured aggregate size distribution.

2.6. Determination of the nucleation parameters

The assessment of nucleation parameters was carried out using the polythermal and isothermal crystallization data from Anuar et al. [9]. In this, the solubility data, calculated from both the gravimetric and dissolution methodologies were used to calculate the solution supersaturation (*S*). The latter was defined as the ratio of the actual solute concentration (*C*) with respect to the material's equilibrium concentration, (*C**) under the same conditions. Using these data, nucleation kinetic parameters based on both isothermal and polythermal analysis methodologies were determined. For the isothermal experiments, the induction time [9] (t_{ind}) was taken to be the elapsed time between the creation of supersaturation and the detection of the solid phase [33–35] with the rate of nucleation (*J*) being determined using classical homogenous nucleation theory [34]. For the polythermal experiments, Nývlt's empirical approach [13,36,37] was used for analysis of the MSZW and the nucleation rate. The background theory and details underpinning methods used is defined in Supplementary Material, section S5.

3. Results and discussion

3.1. Solubility measurements

Data associated with the solubility determination is summarized in Fig. 1. Fig. 1(a) shows the dissolution temperatures of L-isoleucine in water determined at different rates, which shows that the heating rates applied to the solution does not give significant effect to the dissolution temperature. This result justifies the choice of heating rate of 0.7 °C/min in determining other dissolution temperatures for concentrations of 21, 23, 25, 30, 35 g/L in Fig. 1(b). Fig. 1(b) shows the plot of the crystallization temperature, gravimetric solubility and dissolution solubility obtained from this study, together with the illustration of data retrieval for MSZW and supersaturation ratio, S = C/C* (detail equations can be found in Supplementary Material, section S5). The results show that the gravimetric solubility is substantially higher than dissolution solubility. Both data were extensively used by many previous researchers in describing nucleation kinetics and supersaturations of crystallization process [7,11–13,16,17] and in this paper, the impact of using these data, without validity assessment were discussed. The use of these data for MSZW calculation at infinitesimal slow cooling rate (≈0 °C/min) and at 0.7 °C/min were shown in Fig. 1(d). The gravimetric solubility was determined without the effect of heating rates, but for the calculation of this data, the MSZW for gravimetric solubility was determined as the difference between the gravimetric solubility and the crystallization temperature obtained at the respective rates. The result in Fig. 1(d) shows that the use of gravimetric solution for MSZW calculation was underestimated as the MSZW calculated from dissolution solubility (the actual solubility) is always higher. The effect is also apparent for the calculation of supersaturation ratio, in which its value will be consistently underestimated, if calculated using gravimetric solubility. Fig. 1(c) presented in this paper, which was reproduced from Anuar et al. [9] depicts the change of MSZW with cooling/heating rates and concentration. The MSZW is highly dependent on the concentration and rates, and the MSZW used in Fig. 1(d) was obtained from Fig. 1(c). The MSZW at cooling/heating rate, b ≈ 0 °C/min is the intercepts of these lines and the y-axis. Fig. 1(e) shows the van't Hoff plots of this solubility data in comparison to that expected from ideal solubility behaviour.

3.1.1. Measurements using gravimetric methods

The solubility measured by the gravimetric method previously reported [9] was found to be close to that produced by Zumstein & Rousseau [7], whilst assessment of this data by Anuar et al. [9] using the van't Hoff equation has revealed the solubility of isoleucine to be quite low (see Fig. 1(d)). Such a low solubility for L-isoleucine in aqueous solution is perhaps not surprising given the mostly hydrophobic nature of the molecule with only the carboxylate ion being available for solvent binding. Nonetheless, its solubility was found to be substantially higher than predicted based upon ideal solubility behaviour, consistent with strong solvation intermolecular interactions with between L-isoleucine solute molecules and the water [38]. The presence of a change in the slope of the solubility-temperature plot at 45 °C has previously been interpreted as being due to the presence of a metastable polymorphic form (Form B) [9] with both polymorphs being enantiotropically related.

3.1.2. Measurements using dissolution methods

An example of the experimental dissolution data for 42 g/L solute in solution sample is shown in Fig. 2(a) to (d). These show the solutions at 25 °C (a); at 51 °C (1 h) (b); at 51 °C (144 h) (c) and at 64 °C (d). From this it was clear that the expected dissolution temperature [9] based on the gravimetric data of 51 °C was inaccurate as evidenced by crystals still being present even after 144 h at this temperature. Variation in the heating rates used for these measurements was not found to substantially change the measurement of dissolution temperatures, i.e. recording an average temperature, T_{diss} of 64.10 ± 0.15 °C).

3.2. Comparison between solubility parameters derived from gravimetric and dissolution methods

Examination of the solubility data shows that the solubility measured from the dissolution data was lower than that from gravimetric measurements with both 'solubility' lines being found to be substantially higher than that for the ideal solution behaviour, the latter indicative of negative deviation from ideality indicating preferential inter-molecular interactions between L-isoleucine molecules and water [38]. For example, examination of the solubility data reveals that at 25 °C, the ideal solubility is 4.4×10^{-4} g/L in comparison to 34.9 g/L and 23.31 g/L for the gravimetric and dissolution solubilities, respectively. The low overall ideal solubility reflects the unusually high melting point of 288 °C [9] for L-isoleucine, whilst the high differential between ideal and measured solubilities would suggest that the isoleucine molecules must be extremely well solvated. This is perhaps surprising given relatively small hydrophilic surface area for this molecule.

The higher gravimetrically determined 'solubility' would be consistent with the presence of solute aggregation within the solution phase. Presumably an increase in the solution temperature would break up these aggregates and hence facilitate the effective full dissolution of both the crystals and aggregates within the solution. Such a model would suggest that a more accurate value of the solubility would be obtained from the dissolution measurements. The solubility of L-isoleucine measured by using gravimetric method clearly shows two distinct regions (I and II) with a point of inflection at about T = 45 °C suggesting the presence of a phase transformation when in the aggregated solution state. However, further work is clearly needed to fully quantify this effect. The activity coefficient of of this system, as derived from the van't Hoff plots of gravimetric solubility and dissolution solubility from Fig. 1(e), shows (see Supplementary Material S3) that the activity coefficient of L-isoleucine is very low, i.e. within the order of 10^{-4} to 10^{-6}, reflecting its tendency forming aggregates in water and its hydrophobic behaviour in solution. A comparison between the two solubility methods reveals the γ_a value for dissolution method to be higher ($\gamma = 1.2 \times 10^{-5}$ to 8.4×10^{-4}) and further from ideality than that calculated for gravimetric method.

3.3. Comparison between nucleation kinetic parameters derived from gravimetric and dissolution methods

The measurement of accurate solubility data is important for the assessment of metastable zone width (MSZW) and nucleation kinetics.

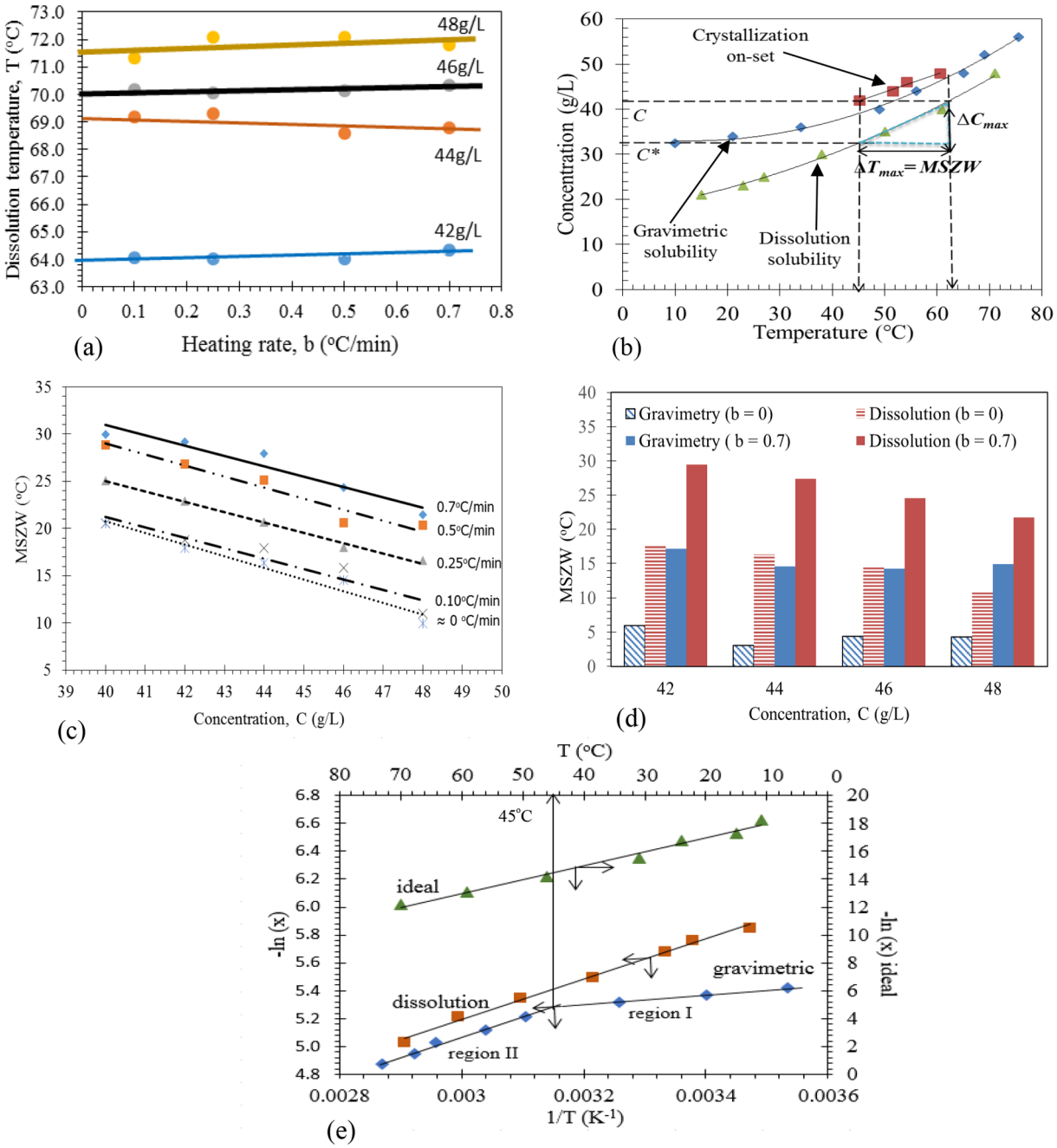

Fig. 1. (a) Heating rates applied shows almost no effect to the dissolving L-isoleucine in water, (b) Crystallization, gravimetric solubility and dissolution curves of L-isoleucine, showing that the solubility derived from dissolution measurements is lower than that from gravimetric measurements for a given temperature, (c) the change of MSZW with rates and concentrations (Reprinted (adapted) with permission from Anuar, N; Wan Daud, W.R.; Roberts, K.J.; Kamarudin, S.K.; Tasirin, S.M. Crystal Growth & Design. 2009, 9: 2852–2862. Copyright (2009) American Chemical Society.) (d) Comparison between calculated MSZW as determined using solubility data obtained from gravimetric [9] and dissolution (this work) experiments. The notation, *b* refers to heating /cooling rate applied to the solution (°C/min), during the dissolution and crystallization process, and (e) the van't Hoff plots of the aqueous solubility of L-isoleucine as determined by gravimetric and dissolution methods together with the ideal solubility.

In this, solubility is often taken as the dissolution of a compound [10,39,40]. Given that this work has shown that the concentration of L-isoleucine as determined using gravimetric methods is higher than that determined using dissolution methods, it is perhaps informative to compare the nucleation parameters obtained from solubility data using these two methods.

Data in Fig. 1(d) (from polythermal crystallization experiment) and Table 1 (from isothermal crystallization experiment) show a comparison between crystallization parameters derived from the gravimetric [9] and dissolution solubility experiments, with the former yielding narrower MSZWs (1.5–3.5 fold) and hence, higher nucleation rates (deviation between 1.9% and 47%, depending on the cooling rates used) than the latter. The calculation carried out using Nývlt equation shows that the order of nucleation, *m* from dissolution data is about 2–3 folds higher than from gravimetric solubility data, whilst the values for the nucleation rate constant, *k* are in the order of between 100 and 1000 folds higher. On the other hand, the use of gravimetric solubility parameters derived from data from isothermal crystallization experiment of L-isoleucine can be expected to clearly affect the estimations of nucleation rate, the critical radius and the number of molecules

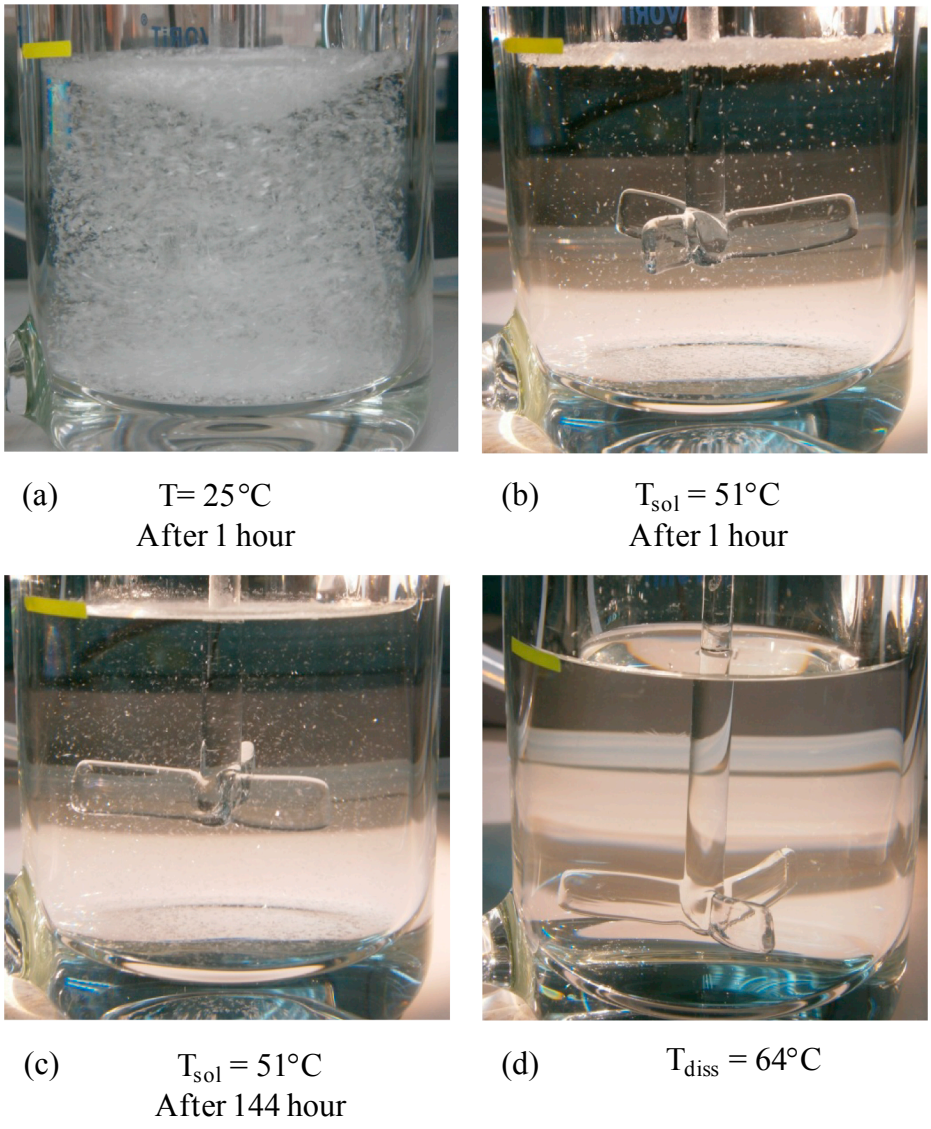

Fig. 2. Visual images of L-isoleucine solution at different temperatures and times, (a) 25 °C after 1 h, (b) 51 °C after 1 h, (c) 51 °C after 144 h highlighting that the crystals did not fully dissolve at solution saturation temperature, T_{sol} 51 °C as determined using gravimetric data; (d) at the measured dissolution temperature, T_{diss} 64 °C.

corresponds to the critical radius.

Comparison between the calculated values for the nucleation rate, critical radius and number of molecules associated to the critical radius for both high and low supersaturations and for starting solution system of 42 g/L are given in Table 1. This analysis shows that for the lower supersaturation (S < 1.29), the calculated nucleation rates based on the gravimetric data are about 2-fold higher than the nucleation rates calculated using dissolution data. For higher supersaturations (S > 1.35), the differences are even greater, typically 200–500-fold higher. Similar discrepancies can be seen in the calculation of the critical cluster sizes (r^*) and number of nuclei per cluster (N^*).

3.4. Characterization of aggregates in solution

L-isoleucine has ammonium and carboxylate hydrophilic groups bonded to the α-carbon, both of which would be expected to have a good affinity with water in contrast to the four hydrophobic alkyl groups. Such a molecular structure would be consistent with L-

Table 1
Calculated values for the nucleation rate, J (from isothermal crystallization experiment) [9], critical radius, r^* and number of molecules associated to critical radius, N^*, and for an initial solution concentration of 42 g/L as calculated from dissolution and gravimetric data at low (S < 1.29) and high supersaturation (S > 1.35).

S	T(°C)	Nucleation rate, J (no./m^3.s)		Critical radius, r^* (Å)		Critical number of molecules, N^*	
		Dissolution data	Gravimetric data	Dissolution data	Gravimetric data	Dissolution	Gravimetric
Low	44.30	2.10×10^{35}	4.52×10^{35}	8.32	10.56	11.48	23.45
	40.00	3.46×10^{35}	7.45×10^{35}	6.82	6.39	6.31	5.20
High	36.80	1.17×10^{33}	5.97×10^{35}	12.24	7.19	36.47	7.39
	34.60	3.16×10^{33}	6.58×10^{35}	11.26	6.44	28.40	5.33

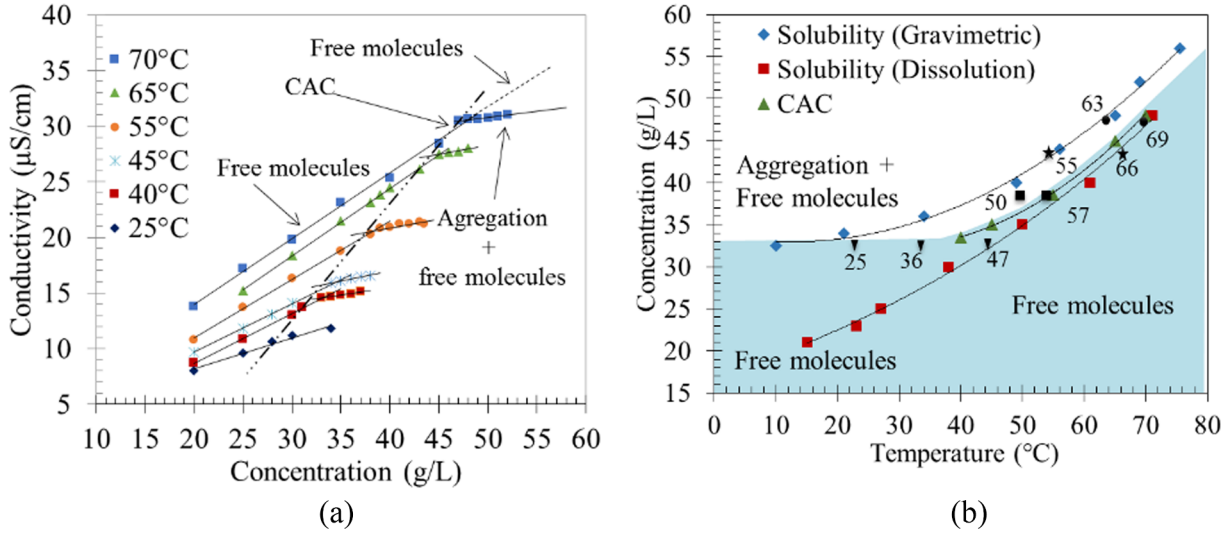

Fig. 3. (a) Conductivity of L-isoleucine solutions at different solute concentrations and temperatures revealing evidence for the molecular aggregation in the solution. (b) Solubility data of L-isoleucine as determined using the gravimetric and dissolution methods. The CAC were also plotted (coloured area region), showing the boundary between the free molecules and the aggregation region. Symbols used in this graph also refer to the temperatures and concentrations for which the size of molecules/aggregates were determined in the solution (see Table 2).

isoleucine forming aggregates in water (or other solvents) due to its amphiphilic nature.

3.4.1. Determination of critical aggregation concentration (CAC)

The conductivity for aqueous L-isoleucine solutions as a function of solute concentration and temperature is shown in Fig. 3(a). The plotted data reveals a distinct change at the CAC in slope and would be consistent with the presence of molecular aggregates in the solution [24,41,42]. CAC inflection points can easily be seen at temperatures above 40 °C. For concentrations above these CAC points it would be expected that aggregates and free molecules would co-exist, whilst below the CAC points, the solute would exist only as free molecules [23] reflecting the fact that the change of slope is caused by the presence of aggregation. However, at 25 °C, regardless of solution concentration (in this case tested for solution between 20 and 35 g/L), no change of slope was observed, which indicates that aggregates do not exist at 25 °C. The conductivity measurement for this temperature for concentrations above 35 g/L could not be measured as this was above the solubility limit for this material. Fig. 3(a) also shows that the conductivity values at every temperature increases when the concentration increases even at a concentration above the CAC point, but with a lower slope. The ionic species contributing to the solution conductivity can be expected to be from the protonated amino group, NH^{3+} and deprotonated carboxyl group, COO^{-} of L-isoleucine. The slight increase in conductivity after the CAC is reached would be consistent with the presence of free single (un-aggregated) molecules in solution [24]. As the concentration increased, the surface layer would be expected to become more saturated with the L-isoleucine molecules and the conductivity would no longer be able to increase. The molecules would be expected to aggregate in order to reduce the surface tension of the solution by shielding the hydrophobic tail the aqueous solution [27]. It is likely that the aggregates formed in solution would be expected to be micelles as concluded from the dilution experiments, based on solution characterization at concentrations which are known to contain aggregates. Upon dilution, the aggregates in the solution disappeared with only the free molecules being detected in the solution.

Fig. 3(b) shows the CAC data overlaid with the solubility. The results show that the CAC points lie within the region between the respective solution concentrations derived from the gravimetric and dissolution measurements. The data mostly lies within a 3-phase region, in which aggregates and free molecules appear to co-exist with the solid crystallographic phase of L-isoleucine, and consistent with the observation that the L-isoleucine crystals were not found to dissolve at temperatures, T_{sol}, as shown in Fig. 2(b) and (c). Such a co-existence probably reflects the amphiphilic nature of the L-isoleucine molecule when the free energy gain through the formation of thermodynamical stable molecular aggregates, which are dispersed in solution is higher than that resulting from solute solvation in an ideal solution environment.

3.4.2. Aggregate size determination

The aggregate size as a function of solute concentration and temperature is given in Table 2 revealing evidence, through the d_{50} data, for a bimodal size distribution as would be, consistent with the presence in solution of both free molecules and molecular aggregates. For example, at a solution concentration of 46 g/L and a temperature of 69 °C, only one size was detected, which is 0.70 nm, whereas at the same concentration but at 63 °C, two sizes were identified, i.e. 0.60 nm and 80 nm. The aggregate sizes determined from Table 2 were also plotted on Fig. 3(b) to highlight the temperature and concentration range for which the free molecules and aggregates were found in the solution. As example, the mean aggregation number, M, calculated using Eq. (1) for the data taken at 63 °C for a concentration of 46 g/L, aggregation sizes of 0.60 nm and 80 nm, were found to be 2 and 31767, respectively, which would be consistent with the presence of a mixture of free molecules (monomers or dimers) and the aggregates typically containing about 1000 molecules in the solution state. The errors of the aggregate size measurement are in the range between 3.4% and 24.5%, respectively. Analysis of aggregate size as a function of reduced concentration at constant temperature revealed evidence for the type of aggregates (e.g. spherical micelle, bilayer, inverse spherical micelles) in the solution. The analysis of the particle size distribution for L-isoleucine solution concentrations of 33 g/L, 38 g/L, 43 g/L and of 48 g/L at temperatures shown in Table 2 is presented in Supplementary Material, section S6. Examination of the 40 g/L data reveals the presence of two size distributions within the solution indicating a mixture of free molecules and aggregates consistent with the CAC value at 50 °C is 36.64 g/L. Similar behaviour has been reported by Ferrer-Tasies et al. [43] who detected multiple sizes of aggregates in solution consistent with the presence of mixed micelles. In contrast, and below the CAC at 32 g/L, only the smaller size distribution was detected in the solution, indicating that only free molecules exist in the solution. Other

Table 2
Dynamic light scattering data highlighting the sizes of molecular aggregates for various solution concentrations and temperatures. The symbols used in this table are in reference to the temperatures and concentrations used to determine the size of the aggregates (see also Fig. 3(b)).

Conc. (g/L)	Symbol	Temp. (°C)	*pH*	pk_{a1}	pk_{a2}	Size at d_{50} (nm)	Aggregation number, M	Condition
46	●$_{69}$	69	4.76	1.60	9.15	0.70	2	Free molecules
	●$_{63}$	63	4.72	1.72	9.20	0.60	2	Free molecules
						80	31,767	+ aggregates
43	★$_{66}$	66	4.75	1.66	9.18	0.65	2	Free molecules
	★$_{55}$	55	4.87	1.88	9.28	0.60	2	Free molecules
						45	10,051	+ aggregates
38	■$_{57}$	57	4.77	1.84	9.26	0.68	2	Free molecules
	■$_{50}$	50	4.83	1.99	9.33	0.60	2	Free molecules
						165	135,135	+ aggregates
33	▼$_{47}$	47	5.48	2.05	9.36	0.60	2	Free molecules
	▼$_{36}$	36	5.45	2.27	9.46	0.63	2	Free molecules
	▼$_{25}$	25	5.47	2.49	9.57	0.63	2	Free molecules

measurements at concentrations 38, 36, 34 and 32 g/L were also found to display similar results and were consistent with the data shown in Fig. 3(b). Overall, the data suggests that the aggregates formed at high concentrations could be easily dissolved into the free molecule forms, which could indicate the aggregates are formed based on the weak inter-molecular interactions such as by a simple hydrogen bond network and/or van der Waals interactions. However, clearly further work is still needed to fully characterize these aggregates in order to fully characterize this behaviour.

3.4.3. Effect of pH on aggregation

The zwitterionic L-isoleucine is a molecule that easily dissociated into three species; the neutral [RH^o] and the ionized [RH$^+$], and [RH$^-$] species, which changes with the solution pH[9]. In this work, the correlation between the pK_{a1} (acidic solution) and pK_{a2} (basic solution); and temperature, T of the solution were found to be linearly related as described by Eq. (2) and (3); respectively,

$$pk_{a2} = -0.0094T + 9.8 \quad (2)$$

$$pk_{a1} = -0.0203T + 3.0 \quad (3)$$

The concentration of these [RH^o] species which have both a negative charge from carboxyl group and a positive charge from the amino group in its molecule structure is the dominant species at pH 7. The anionic [RH$^-$] species has a negative charge carboxyl group in its molecule and is dominant in an alkali environment, whilst the cationic [RH$^+$] species is dominant in acidic solutions. Previous work [9] has shown that the species dissociation behavior is temperature-dependent and that increasing the temperature changes the species equilibria, e.g. promoting the dissociation of [RH$^+$] to [RH^o], and [RH^o] to [RH$^-$]. Measurements of the solution pH for the various concentrations, which were defined by a known aggregate size distribution and shown in Fig. 4, revealed that lower pH values were recorded for solutions containing both free molecules and aggregates, whilst for solutions containing only free molecules, the pH values were higher. This would be consistent with a reduction in the concentration of neutral [RH°] species as free molecules associated with the aggregation into molecular clusters. The analysis of species distribution with temperature and concentration showed that the neutral [RH^o] was the dominant species within the temperature and concentration range examined in this work, with respect to the ionized cationic [RH$^+$] and anionic [RH$^-$] species. The graphical representation of these distributions is shown in Fig. 5 highlighting the inter-relationship between the species concentrations, solute concentration and temperature as calculated from the Henderson-Hasselbach equation. The variation of pH and the *pka* values with temperature are given in Table 2. However, it is interesting to note that the concentration of the [RH^o] species for the free molecules increases as a function of solution the concentration and temperature of

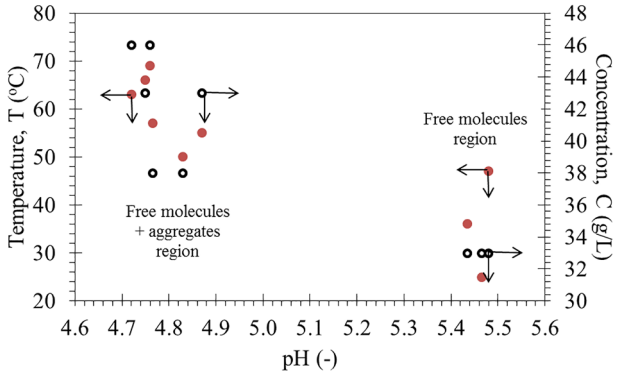

Fig. 4. The change of solution pH with temperature (closed red circles) and concentration (open black circles) shows two distinct pH ranges consistent with the region with only free molecules existing at a higher solution pH than that containing both free molecules and aggregates. (For interpretation of the references to colour in this figure legend, the reader is referred to the web version of this article.)

the increases. This is consistent with the self-assembly of free molecules forming aggregates associated with concomitant reduction in their concentration in solution. On the other hand, the concentration of free molecules for the [RH$^+$] species in the solution remains higher than that of the [RH$^-$] species, regardless the change of concentration and temperature of the solution. In the region where both free molecules and aggregates co-exist, the amount of aggregated [RH$^+$] species was always found to be higher than the amount of positively charged free molecules. The [RH$^-$] species, which usually dissociated from the [RH^o] in alkaline solution, remained, as expected, at low concentration within the solution albeit with a small reduction in its concentrations as it moved from the free molecule to the molecular aggregation region. Reduction in solution pH in the aggregated molecular state is consistent with the aggregates being formed from the [RH^o] neutral species suggesting, that this compound might crystallize via a 2-step nucleation process. However, this theory has yet to be proven within the vicinity of investigation carried out in this work and thus we are not able to confirm with a high degree of certainty that this system deviates the classical nucleation theory.

3.5. Solute aggregation implications for the nucleation mechanism

Whilst these observations of the aggregation of neutral [RH]° solute species, as reported here, have been based upon measurements made under equilibrium conditions, their presence might also be indicative with a two-step nucleation mechanism [44] given the aggregates seem to be mostly composed of neutral species. However, this comment

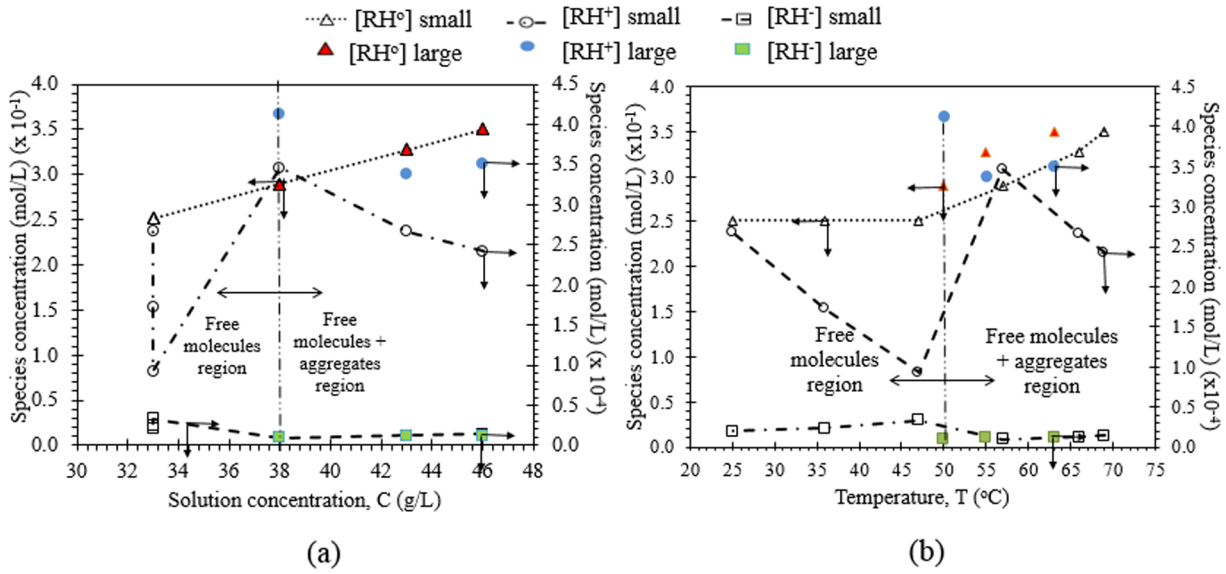

Fig. 5. Distribution of species concentration in the solution showing at various (a) concentrations and (b) temperatures with aggregated species (denoted as 'large' in the legend) having significant differences in concentration with respect to the free molecules (denoted as 'small' in the legend).

should be treated with caution until detailed structuro-kinetic studies can be carried out in order to map out the molecular aggregation state during cooling from the under-saturated solution state through to the MSZW boundary in order to gain a greater insight to the observed phenomena.

4. Conclusions

A comparison between solubility data for L-isoleucine obtained using both gravimetric and dissolution methods revealed significant differences with the former indicating a higher value. Measurements of the CAC revealed that this observation was consistent with a degree of solute aggregation in the slurried state. Analysis using dynamic light scattering and pH measurements were consistent with the slurried aggregates comprising neutral species in the size range 45–165 nm. Solutions at higher solute concentrations and temperature were found to produce lower solution acidity and to promote aggregate formation. These observations might be consistent with a 2-step nucleation process for this material, whereby molecular aggregates formed in solution formed incipient nuclei for subsequent crystallization. However, further investigation needs to be carried out to confirm this theory. The implication of deriving nucleation kinetics data using solubility derived from the two solubility methods suggest significant differences in MSZW and nucleation rates implying that caution might be needed when using gravimetric solubility data for the characterisation of crystallization kinetics for systems which display a propensity for solute aggregation, particularly for amphiphilic molecules. For such case, dissolution solubility should be treated as an effective solubility, instead of gravimetric solubility.

Acknowledgements

The authors would like to express their gratitude to the Ministry of Higher Education, Malaysia for funding this work which was carried out at Universiti Teknologi MARA, Malaysia in collaboration with the University of Leeds, UK. One of us (NSMA) would like to thank the Ministry of Higher Education, Malaysia for the sponsorship of her PhD studies. This work is part of research grant 600-RMI/FRGS 5/3(92/2013) and 600-RMI/MyRA 5/3/BESTARI (023/2017). One of us (KJR) also gratefully acknowledges the Engineering and Physical Sciences Research Council (EPSRC, UK) for the funding of nucleation research at Leeds through a Critical Mass project in collaboration with the University of Manchester (grant references EP/IO14446/1 and EP/IO13563/1).

Appendix A. Supplementary material

Supplementary data to this article can be found online at https://doi.org/10.1016/j.jcrysgro.2019.04.019.

References

[1] B. Bouillot, S. Teychené, B. Biscans, Fluid Phase Equilib. 309 (2011) 36–52.
[2] N.F. Zolkiflee, A.B. Majeed, M.M. Affandi, Int. J. Res. Pharm. Sci. 8 (1) (2017) 90–102.
[3] I. Hahnenkamp, G. Graubner, J. Gmehling, Int. J. Pharm. 388 (2010) 73–81.
[4] S. Baluja, E.A. Alnayab, A. Hirapara, J. Mol. Liq. 238 (2017) 84–88.
[5] R. Thakuria, A. Delori, W. Jones, M.P. Lipert, L. Roy, N. Rodríguez-Hornedo, Int. J. Pharm. 453 (2013) 101–125.
[6] F. Ab Rahman, S. Abd Rahim, C.C. Tan, S.H. Low, N.A. Ramle, Int. J. Chem. Eng. Appl. 8 (2) (2017) 136–140.
[7] R.C. Zumstein, R.W. Rousseau, Ind. Eng. Chem. Res. 28 (8) (1989) 1227–1231.
[8] G. Sherman, S. Shenoy, R.A. Weiss, C.A. Erkey, Ind. Eng. Chem. Res. 39 (2000) 846–848.
[9] N. Anuar, W.R. Wan Daud, K.J. Roberts, S.K. Kamarudin, S.M. Tasirin, Cryst. Growth Des. 9 (2009) 2852–2862.
[10] S. Hassan, F. Adam, M.R. Abu Bakar, S.K. Abdul Mudalip, J. Saudi Chem. Soc. (2018), https://doi.org/10.1016/j.jscs.2018.07.002 Article in Press.
[11] M. Rabesiaka, C. Porte, J. Bonnin-Paris, J.-L. Havet, J. Cryst. Growth 332 (2011) 75–80.
[12] L.A. Smith, A. Duncan, G.B. Thomson, K.J. Roberts, D. Machin, G. McLeod, J. Cryst. Growth 263 (1–4) (2004) 480–490.
[13] L.A. Smith, K.J. Roberts, D. Machin, G. McLeod, J. Cryst. Growth 226 (1) (2001) 158–167.
[14] K. Sangwal, J. Cryst. Growth 311 (16) (2009) 4050–4061.
[15] L. Nemdili, O. Koutchoukali, M. Bouhelassa, J. Seidel, F. Mameri, J. Ulrich, J. Cryst. Growth 451 (2016) 88–94.
[16] S. Rama, C. Surendra Dilip, R.N. Perumal, J. Cryst. Growth 409 (2015) 32–38.
[17] K. Selvaraju, K. Kirubavathi, N. Vijayan, S. Kumararaman, J. Cryst. Growth 310 (11) (2008) 2859–2862.
[18] N. Kobko, M. Marianski, A. Asensio, R. Wieczorek, J.J. Dannenberg, Comput. Theor. Chem. 990 (2012) 214–221.
[19] R. Bordes, K. Holmberg, Adv. Coll. Interf. Sci. 222 (2015) 79–91.
[20] J. Israelachvili, Intermolecular and surface forces, 3rd Ed., Academic Press, London, 2011.
[21] B.W. Ninham, P.Lo Nostro, Molecular forces and self-assembly in colloid, nano sciences and biology, Cambridge University Press, Cambridge, 2010.
[22] C. Tandford, The hydrophobic formation effect of micelles and biological membranes, 2nd Ed., Wiley, New York, 1980.
[23] T. Chakraborty, I. Chakraborty, S. Ghosh, Arabian J. Chem. 4 (3) (2011) 265–270.
[24] A. Dominguez, A. Fernandez, N. Gonzalez, E. Iglesias, L. Montenegro, J. Chem. Educ. 74 (10) (1997) 1227.
[25] R. Zana, Dynamics of surfactant self-assemblies: micelles, microemulsions, vesicles

and lyotropic phases, 1st Ed., CRC Press, 2005.
[26] L.L. Schramm, Surfactants: fundamentals and applications in the petroleum industry, Cambridge University Press, 2000.
[27] A.T. Florence, D. Attwood, Physicochemical principles of pharmacy, 4th Ed., Pharmaceutical Press, 2006.
[28] D. Dressler, H. Potter, Discovering enzymes, Scientific American Library, New York, 1991.
[29] H. Matsuo, Y. Suzuki, S. Sawamura, Fluid Phase Equilib. 200 (2002) 227–237.
[30] H.A.B. Hasanuddin, M.M. Affandi, M. Salama, M. Tripathy, Orient. J. Chem. 30 (3) (2014) 1119–1123.
[31] National Center for Biotechnology Information. PubChem Compound Database; CID = 6306, (accessed Oct. 5, 2016). < https://pubchem.ncbi.nlm.nih.gov/compound/6306 > .
[32] D.A. Skoog, D.M. West, F.J. Holler, Fundamentals of analytical chemistry, 5th Ed, Brooks Cole, California, 1996.
[33] S.A. Kulkarni, S.S. Kadam, H. Meekes, A.I. Stankiewicz, J.H. ter Horst, Cryst. Growth Des. 13 (6) (2013) 2435–2440.
[34] S. Ghader, M. Manteghian, M. Kokabi, R.S. Mamoory, Chem. Eng. Technol. 30 (2007) 1129–1133.
[35] E.M. Flaten, M. Seiersten, J.-P. Andreassen, Chem. Eng. Res. Des. 88 (12) (2010) 1659–1668.
[36] K. Sangwal, J. Cryst. Growth 312 (2010) 3316–3325.
[37] K. Sangwal, CrystEngComm. 13 (2011) 489–501.
[38] R.J. Davey, J.W. Mullin, M.J.L. Whiting, J. Cryst. Growth 58 (1982) 304–312.
[39] C. Beck, S.V. Dalvi, R.N. Dave, Chem. Eng. Sci. 65 (2010) 5669–5675.
[40] N. Gherras, G. Fevotte, J. Cryst. Growth 342 (2012) 88–98.
[41] M. Yan, B. Li, X. Zhao, Food Chem. 122 (4) (2010) 1333–1337.
[42] A. Zdziennicka, K. Szymczyk, J. Krawczyk, B. Jańczuk, Fluid Phase Equilib. 322–323 (2012) 126–134.
[43] L. Ferrer-Tasies, E. Moreno-Calvo, M. Cano-Sarabia, M. Aguilella-Arzo, A. Angelova, S. Lesieur, S. Ricart, J. Faraudo, N. Ventosa, J. Veciana, Langmuir 29 (2013) 6519–6528.
[44] P.G. Vekilov, J. Cryst. Growth 275 (2005) 65–76.